Growth and mechanical properties of a MoC precipitate at a Mo grain boundary: An *ab initio* density functional theory study

Rebecca Janisch
Institut für Werkstoffwissenschaften, Universität Erlangen-Nürnberg, Martensstrasse 5, 91058 Erlangen, Germany

Christian Elsässer
Fraunhofer-Institut für Werkstoffmechanik, Wöhlerstrasse 11, 79108 Freiburg, Germany

(Received 30 July 2007; revised manuscript received 19 November 2007; published 14 March 2008)

Atomic-scale stages of the growth of an interfacial precipitate film of tetragonal molybdenum carbide at a Σ5 (310) [001] symmetrical tilt grain boundary in body-centered cubic molybdenum were investigated by means of atomistic supercell calculations on the basis of *ab initio* density functional theory. The structural development of the precipitate with increasing carbon concentration is analyzed qualitatively and quantitatively. The structurally optimized atomistic model for the fully developed precipitate is compared to experimental high-resolution images from transmission electron microscopy. Characteristic interface energies are calculated to evaluate the influence of the precipitate on the mechanical stability of the material. Finally, an atomic-scale twinning mechanism in the MoC precipitate is proposed.

DOI: 10.1103/PhysRevB.77.094118 PACS number(s): 68.35.−p, 68.55.A−, 71.15.Mb

I. INTRODUCTION

The macroscopic behavior of polycrystalline materials is vitally influenced by the properties of grain and phase boundaries in their microstructures. The cohesion at these internal boundaries affects the hardness, plastic deformability, and fracture toughness of the material and it can be enhanced or decreased by point defects, such as segregated impurities, by dislocations, or by precipitated second phases. These effects are particularly strong in the body-centered cubic (bcc) transition metals, which have very interesting high-temperature applications. However, these metals suffer from a strong tendency to grain boundary embrittlement. There is a strong influence of impurities on this embrittlement, for the worse or for the better.[1] Thus, it is desirable to optimize the materials properties if one understands the mechanisms and effects of solid solution, segregation, and precipitation processes related to the different impurities. We contribute to this effort with our study of precipitation of molybdenum carbide at the Σ5 (310)[001] symmetrical tilt grain boundary (STGB) in Mo.

The Σ5 STGB in pure Mo has been studied extensively before, both experimentally[2–4] and theoretically.[5–8] It is a favorite case study in the long-term discussion of the meaning and the way of determination of the translational geometric degrees of freedom of such a grain boundary, as well as of the influence of defects thereon. Our own work on the influence of segregated impurities on grain boundary cohesion in Nb and Mo (Refs. 1 and 9) is the starting point of the study presented here. The motivation to choose this particular system, C at the Σ5 (310)[001] STGB in Mo, was many-fold. First of all, carbon is an abundant impurity element that can hardly be avoided in the real material. Second, it has been observed to have a strengthening effect on Mo (Ref. 10); thus, it is desirable to understand the underlying mechanism and to investigate to what extent this is transferable to other elements. Furthermore, an extensive high-resolution transmission electron microscopy (HRTEM) study of Pénisson *et al.*[2] on this grain boundary provides us with experimental details for comparison.

In the following, the experimental procedure and the results of Pénisson *et al.* are summarized in Sec. II. The computational method employed in the study at hand is introduced in Sec. III. The initial stage of the precipitation is modeled by calculations with 1–4 ML (monolayer) of C atoms at the grain boundary of Mo. The calculation of the characteristic interface energies is explained in Sec. IV. The results are presented in Sec. V. Atomistic structures and characteristic energies of a fully developed tetragonal MoC film at the Σ5 STGB in Mo are investigated in Sec. VI. Summary and conclusions are presented in Sec. VII.

II. SUMMARY OF PRECEDING EXPERIMENTAL FINDINGS

Pénisson *et al.* performed HRTEM on the Σ5 STGB in a Mo bicrystal before and after carburization heat treatments.[2] By choosing different carburization conditions, the authors obtained samples with different C contents, and they observed different intra- and intergranular MoC_x phases. Of particular interest is a substoichiometric tetragonal phase occurring both as inter- and intragranular precipitates at low temperatures, when the precipitation took place below the temperature of carburization. From the measured lattice parameters ($a=0.305$ nm, $c=0.406$ nm, i.e., $c/a=1.33$), Pénisson *et al.* derived a C concentration of $x\approx 0.4$. This kind of tetragonal precipitate has been observed earlier by Lepski and Burck[11,12] in the form of intragranular, disk shaped particles.

At the Σ5 STGB, the orientation relationship between MoC_x and Mo is[2]

$$[001]_{\mathrm{Mo}} \| [010]_{\mathrm{MoC}_x},$$

$$(310)_{\mathrm{Mo}} \| (103)_{\mathrm{MoC}_x}, \quad (1)$$

on one side of the precipitate film. In the following, we call this phase boundary as "interface I." On the other side, the precipitate film is limited by a phase boundary called "interface II" with the orientation relationship

$$[001]_{\mathrm{Mo}} \| [010]_{\mathrm{MoC}_x},$$

$$(\bar{3}\bar{1}0)_{\mathrm{Mo}} \| (103)_{\mathrm{MoC}_x}. \quad (2)$$

At interface I, the tilt angle is approximately 40° and thus close to that of the original Σ5 STGB (36.89°). At interface II, the crystallographic planes in MoC_x continue with a small deviation of approximately 6° into the Mo grain.

From the experimental results, it can be deduced that the segregation of C to the Σ5 STGB in Mo is taking place via octahedral interstitial sites. The C atoms lead to a tetragonal distortion of the cubic Mo lattice and at higher C concentrations to the precipitation of tetragonal MoC_x at the grain boundary. In the following sections, our computational method and the atomistic modeling strategy, which we used to describe the process of segregation and precipitation, are explained.

III. COMPUTATIONAL METHOD

Our results for structures and energies were obtained by means of the *ab initio* mixed-basis pseudopotential method,[13–19] which is based on the density functional theory (DFT). The local density approximation was made for exchange correlation.[20] Norm-conserving ionic pseudopotentials were used for the core-valence interactions,[21,22] and the pseudo-wave-functions were represented by a mixed basis consisting of plane waves and local functions.[14,15]

A base-centered orthorhombic supercell containing 22 atoms (20 Mo plus 2 C) was employed as a starting model for the Σ5 (310)[001] STGB with segregated C atoms, which has already been used and validated in previous investigations of the pure STGB in the bcc metals[7,8,23] and of the influence of segregated interstitial impurities.[1,9] For the Brillouin zone integrations, we applied a $4\times8\times2$ k-point mesh that was constructed following the scheme of Moreno and Soler.[24] The resulting k-point density was that of an $8\times8\times8$ k-point mesh for a unit cell of bulk bcc Mo. A Gaussian smearing of 0.004 Ry was used. The cutoff energy for the plane waves in the basis set was $E_{pw}=16$ Ry. The local functions, five per atom with d symmetry for Mo and three per C atom with p symmetry, were confined to spheres centered at host-metal lattice sites $[r_{lo}(\mathrm{Mo})=2.00$ bohr] and at impurity sites $[r_{lo}(\mathrm{C})=1.80$ bohr]. The atomic units for energy and length used in this context of computational settings are 1 Ry=13.606 eV=2.18×10^{-18} J and 1 bohr=0.0529 nm.

IV. INTERFACE ENERGIES

First, we want to determine whether at the Σ5 STGB in Mo a tetragonal carbide precipitate of the kind described above will grow in an asymmetrical fashion with respect to the interface, leading to a crystalline MoC phase sandwiched between the two misoriented Mo grains, or in a symmetrical way, such that there will be a STGB inside the MoC phase in the end. The resulting interfaces will have different energies and different mechanical properties.

The precipitation process was modeled by adding one C atom per interfacial unit cell at a time[36] and calculating the interface energy,

$$\gamma = \frac{E_{tot,GB}^{\mathrm{Mo}+n\mathrm{C}} - N\mu_{\mathrm{Mo}} - n\mu_{\mathrm{C}}}{A}, \quad (3)$$

as well as the segregation energy

$$E_{seg} = \frac{E_{tot,GB}^{\mathrm{Mo}+n\mathrm{C}} - E_{tot,GB}^{\mathrm{Mo}+(n-2)\mathrm{C}} - 2\mu_{\mathrm{C}}}{A}, \quad (4)$$

where $E_{tot,GB}^{\mathrm{Mo}+n\mathrm{C}}$ is the total energy of the grain boundary supercell with n carbon atoms at the interface, $E_{tot,GB}^{\mathrm{Mo}+(n-2)\mathrm{C}}$ is the total energy of the preceding configuration, and A is the total interface area in the supercell (two times the cross-sectional area of the supercell parallel to the interface). For the chemical potential of molybdenum μ_{Mo} the total energy of a Mo atom in the bcc phase was chosen. The chemical potential of carbon μ_{C} was varied in the range between the energy of a C atom in the cubic diamond phase and that of an interstitial C atom in bcc Mo,

$$\mu_{\mathrm{C}}^{diamond} \leq \mu_{\mathrm{C}} \leq \mu_{\mathrm{C}}^{interstitial}, \quad (5)$$

to mimick the variation of the partial pressure of C from C-poor (low chemical potential) to C-rich (high chemical potential) conditions, respectively, in experimental investigations. The relationship between partial pressure and chemical potential as well as the computational equivalent of a chemical potential is, for instance, discussed in Ref. 25. The value for $\mu_{\mathrm{C}}^{interstitial}$ was determined as the total energy of a $Mo_{10}C_1$ supercell of bulk bcc Mo with one interstitial C, corresponding to one of the two Mo grains in the supercell of the Σ5 STGB. The value for $\mu_{\mathrm{C}}^{diamond}$ was estimated as the total energy of bulk cubic diamond C, which is almost the same as that of bulk graphite C. In addition to γ and E_{seg}, the work of separation was calculated for the different interfaces occurring inside the fully grown precipitate (a grain boundary) or at the precipitate/matrix phase boundary (interface I or interface II). It is defined as the total energy difference per interface area between the two free surfaces and the interface, with all atomic positions being relaxed, but the supercell parameters parallel to the interface kept fixed[26] at values of the surrounding matrix of bulk bcc Mo,

$$W_{sep} = \frac{E_{tot,FS} - E_{tot,IF}}{A}, \quad (6)$$

where "IF" denotes the interface (either a grain boundary or a phase boundary) and "FS" the according free surfaces. The quantity W_{sep} has the advantage of being independent of μ_{C}.

V. "NUCLEATION" AND "GROWTH" OF THE PRECIPITATE

Starting with the mirror-symmetric configuration of the Σ5 STGB in Mo with one segregated C atom per interfacial

TABLE I. Grain boundary energies γ according to Eq. (3), the same with respect to the energy of the pure Mo STGB, $\Delta\gamma$, and segregation energies E_{seg} per C atom according to Eq. (4) for different C concentrations and distributions at the $\Sigma 5$ grain boundary in Mo. The values are obtained with a chemical potential $\mu_C = \mu_C^{diamond}$ for C in the diamond phase. The different configurations are described in detail in the text.

n	Label	γ (J/m^2)	$\Delta\gamma$ (J/m^2)	E_{seg} (J/m^2)
0	Pure	1.807		
1	A	1.297	−0.510	−2.136
2	B1	2.757	0.950	+0.731
	B2	1.148	−0.659	−0.077
	B3	3.460	1.653	+1.051
3	C1	2.251	0.444	+0.897
	C2	2.561	0.754	+0.710
	C3	5.247	3.440	+1.280
	C4	3.976	2.169	+1.412
4	D1	6.762	4.955	+2.261
	D2	4.954	3.147	+1.197

unit cell, the concentration of C at the grain boundary was increased atom by atom. For each concentration, a variety of possible sites for C had to be probed. For all the different cases, all atomic positions were relaxed until the forces on the atoms were negligible (less than 10^{-3} Ry/bohr). Subsequently, the preference of different C positions was evaluated by comparing the grain boundary energies γ as well as the segregation energies E_{seg} of the the fully relaxed systems.

Important configurations will now be discussed in detail. The results for γ, obtained by using the chemical potential $\mu_C = \mu_C^{diamond}$ of C in the cubic diamond phase in Eq. (3), are summarized in Table I.

The preferred site of the first C atom put at the interface has been determined in our previous study[1] (see Fig. 2 therein). It is the center of a trigonal prism formed by the surrounding metal atoms, and it leads to a concentration of 1 ML of C at the grain boundary. In the following, this configuration is called "A." The segregation energy for this case A is strongly negative for all μ_C values in the range given by relation (5), which means that the interface is attractive for the segregation of interstitial atoms. Concomitantly, the interface energy is lowered by the presence of C at the grain boundary (cf. Table I). Furthermore, as explained in detail in Ref. 1, the C atoms also increase the grain boundary cohesion by forming bonds with covalent character to the neighboring host-metal atoms, as well as by increasing the strength of the metal-metal bonds across the interface.

For the segregation of a second C atom, the first possibility (B1) is an octahedral site in the Mo lattice between two Mo atoms in the crystal plane meeting the grain boundary at an angle of 18°, as shown in Fig. 1(a). The second possibility (B2) is the corresponding site in the crystal plane meeting the interface at an angle of 108°, cf. Fig. 2(a). In both cases, the C is distributed in two times 1 ML of C in adjacent

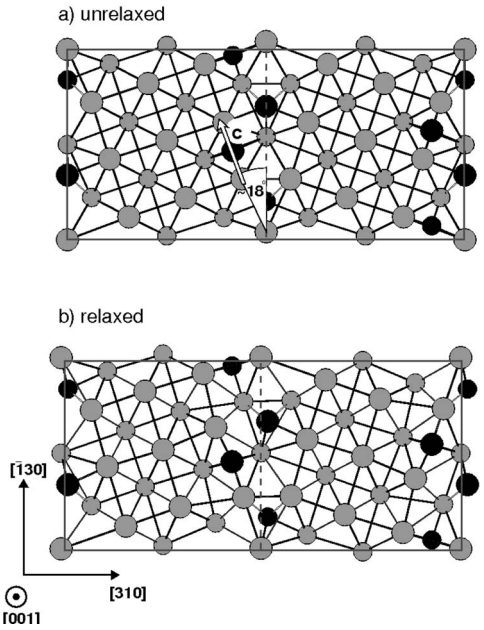

FIG. 1. Possibility B1 of putting two C atoms at the Mo $\Sigma 5$ STGB: (a) unrelaxed supercell and (b) after relaxation of all atomic positions. The large atoms are positioned in the paper plane, and the small atoms in the next layer in the [001] direction. Mo atoms are gray, and C atoms black. The arrow **c** indicates the c axis of a tetragonal distortion, and the angle 18° its deviation from the geometric interface plane.

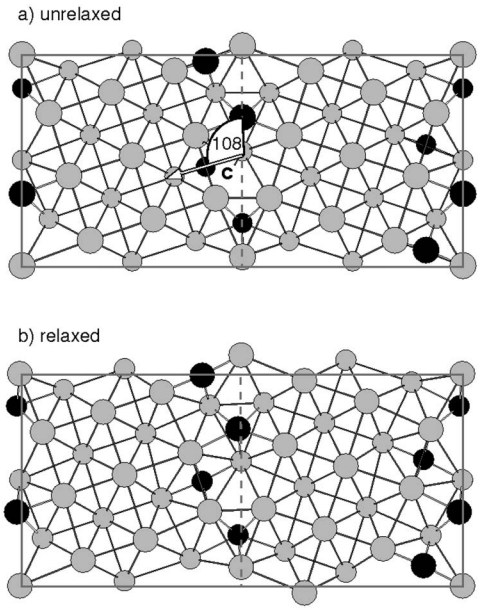

FIG. 2. Possibility B2 of putting two C atoms at the Mo $\Sigma 5$ STGB: (a) unrelaxed supercell and (b) after relaxation of all atomic positions. The large atoms are positioned in the paper plane, and the small atoms in the next layer in the [001] direction. Mo atoms are gray, and C atoms black. The arrow **c** indicates the c axis of a tetragonal distortion, and the angle 108° its deviation from the geometric interface plane.

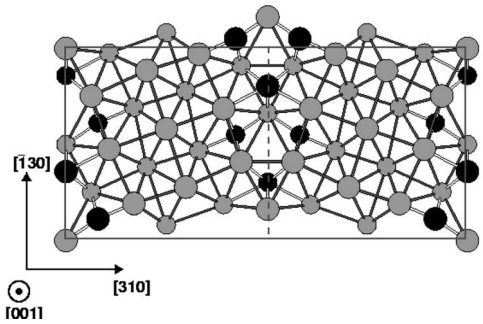

FIG. 3. Symmetrical MoC precipitate (C1) formed by the C atoms at the Mo Σ5 STGB, in a supercell after relaxation of all atomic positions. The large atoms are positioned in the paper plane, and the small atoms in the next layer in the [001] direction. Mo atoms are gray, and C atoms black.

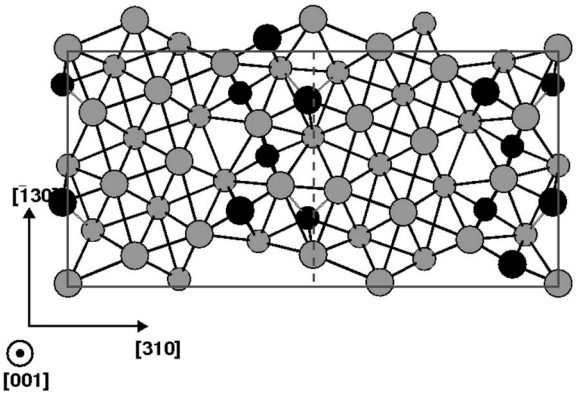

FIG. 4. Asymmetrical MoC precipitate (C2) formed by the C atoms at the Mo Σ5 STGB, in a supercell after relaxation of all atomic positions. The large atoms are positioned in the paper plane, and the small atoms in the next layer in the [001] direction. Mo atoms are gray, and C atoms black.

crystal planes. The first case leads to an expansion of the structure mainly parallel to the interface, and the second mainly perpendicular to it. The third possibility, B3, is to place the second C atom in the interface plane as well, leading to a bilayer of C at the grain boundary. Case B2 is most favorable, still exhibiting a negative segregation energy and leading to a lower interface energy than in the pure case. B1 and B3 exhibit positive segregation energies while the interface energies go up. This correlation between segregation and interface energies follows the Gibbs absorption theorem[27] and has also been observed at grain boundaries before.[28] For example, Hondros measured a decreasing average grain boundary energy with increasing concentration of P in polycrystalline bcc Fe, up to a concentration of 1/3 of a monolayer of P at the interfaces.[29] Our results show that for C in bcc Mo, the saturation concentration at the Σ5 STGB can be higher, at least 1 ML. It can be increased even further by increasing the chemical potential from $\mu_C^{diamond}$ to $\mu_C^{interstitial}$, where all segregation energies are shifted to negative values (see Fig. 5 below and discussion at the end of this section).

Figures 1(b) and 2(b) show the relaxed supercells for cases B1 and B2. In both cases, the C atom causes a rather localized tetragonal distortion along the c axis marked in Figs. 1(a) and 2(a). The pure Mo grain on the other side of the interface remains unaffected, showing that the grain boundary can absorb a considerable amount of elastic energy. Together with the fact that a tetragonal lattice distortion in this orientation does not destroy the coherency of the interface, this explains why configuration B2 turns out to be the most favorable one.

In the next step, a third C atom was inserted. The possibilities probed were C1, starting from B2, opposite to the previously inserted C atom on the other side of the grain boundary (symmetrical growth), as shown in Fig. 3; C2, starting from B2, next to the previously inserted one inside the same grain (asymmetrical growth), as shown in Fig. 4; C3, starting from B1, in the grain boundary plane (not shown); C4, starting from B2, in the grain boundary plane (not shown). The resulting interface energies and segregation energies are given in Table I. For configurations C1 and C2, in which another layer of MoC is added to the precipitate, the interface energies are higher than that of the pure Mo STGB and the segregation energies are positive, but the absolute value of γ is still rather low. C3 and C4, however, in which the concentration of C at the grain boundary is increased from a monolayer to a bilayer, are much higher in energy. Obviously, an increased bulk concentration of C on one side of the grain boundary does not increase the saturation concentration at the interface.

This can change if the total concentration of C in the supercell is increased. For adding a fourth C atom to the interfacial precipitate, configurations C1 and C2 were chosen as starting points, leading to configurations D1 (symmetric) and D2 (asymmetric). Again, the grain boundary energies increase considerably with respect to the pure grain boundary. Note, however, that with the higher C concentration at both sides of the interface, configuration D2 is lower in energy than C3. This demonstrates that the saturation concentration of C at the Σ5 STGB in Mo can be increased by increasing the bulk concentration, i.e., by increasing the chemical potential of C in Eqs. (3) and (4). This is demonstrated in Fig. 5. Shown is the interface energy difference $\Delta\gamma$ (circles) with respect to the pure Mo STGB as a function of the carbon concentration for the respectively most favorable configuration, calculated with $\mu_C^{diamond}$. With the first 2 ML of C at the interface, the energy is lowered. From the third monolayer (the symmetric case C1), the energy rises above the energy of the pure Mo grain boundary. Note that while a symmetric arrangement of C (or MoC) around the GB is favored with 2 and 3 ML of C (B2 and C1), this trend is reversed and an asymmetric arrangement is preferred in the next step (D2). The comparison of the interface energy difference $\Delta\gamma$ with the segregation energy E_{seg}, which is also displayed in Fig. 5 (squares), shows that the behavior follows the Gibbs absorption theorem, i.e., as long as the interface energy is lowered by C, the grain boundary is attractive for C, as indicated by the negative sign of E_{seg}, for low C partial pressures (i.e., with $\mu_C \geq \mu_C^{diamond}$, upper curve). For higher C partial pressures (i.e., with a higher $\mu_C \leq \mu_C^{interstitial}$, lower curve), the clear link to the Gibbs absorption theorem is lost

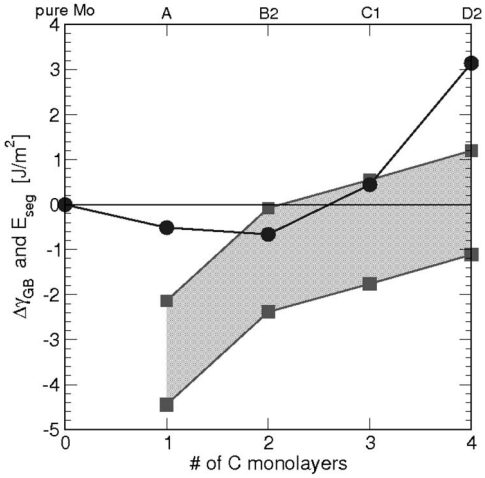

FIG. 5. Interface energy difference $\Delta\gamma$ (circles) and segregation energy E_{seg} per C atom (squares) of the $\Sigma 5$ STGB in Mo as a function of C concentration. For the segregation energy, the chemical potential of C has been varied between $\mu_C^{interstitital}$ (lower curve) and $\mu_C^{diamond}$ (upper curve).

since now the segregation energy is always negative. However, this plot demonstrates that under experimental conditions, the growth of the precipitate does not necessarily stop after the second monolayer, as already mentioned above.

VI. THE MoC PRECIPITATE: THREE NEW INTERFACES

Our study of the nucleation and growth of the precipitate shows the tendency of the carbide phase to grow with the tetragonal distortion forming an angle of 108° to the grain boundary plane, in agreement with the experimental finding in Ref. 2. The spatial extent of the precipitate, as well as the concentration of C in the grain boundary plane, can be varied by means of the carbon chemical potential μ_C. However, from our results obtained so far, the symmetry of the precipitate with respect to the interface remains ambiguous: Will a thicker Mo-C precipitate film preserve the mirror symmetry of the original Mo STGB by forming a MoC STGB inside (as in Fig. 3, see also Fig. 10) or not (as in Fig. 4, see also Fig. 6)? Thus, we now turn to the end of the precipitation process and evaluate the different possible results. As mentioned above, these are either a single crystalline MoC phase sandwiched between the two original Mo grains, bordered by interfaces I and II described in Sec. II, or a MoC phase that contains a STGB and is bordered by two interfaces II. Atomistic models for these three interfaces were constructed, relaxed, and characterized, as described in the following.

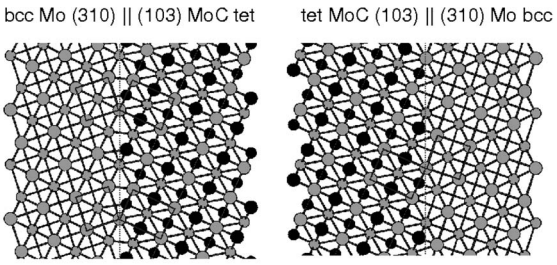

FIG. 6. Model interfaces "I" and "II" for the precipitate of bct MoC at the $\Sigma 5$ STGB of bcc Mo. The large atoms are positioned in the paper plane, and the small atoms in the next layer in the [001] direction. Mo atoms are gray, and C atoms black.

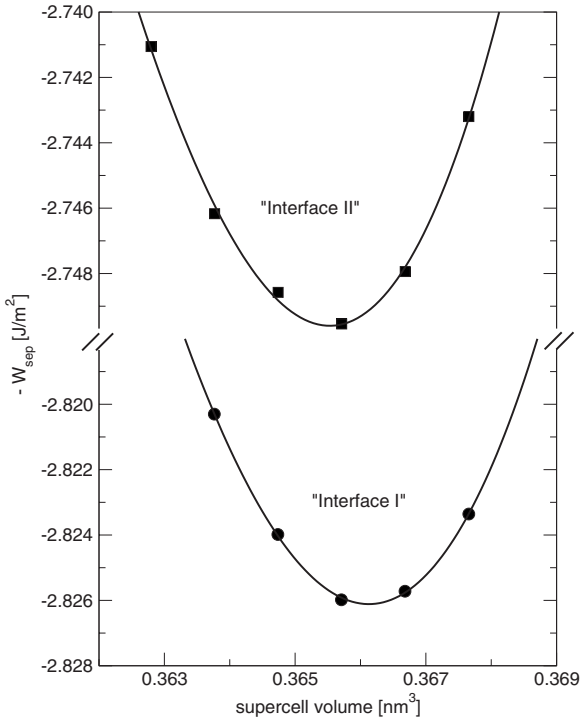

FIG. 7. Negative work of separation $-W_{sep}$ of interfaces I and II for volume expansion along [310] with relaxation of all atomic positions.

A. Model structures: The Mo/MoC interfaces

To model the interfaces between the tetragonal MoC precipitate and the surrounding bcc Mo matrix, one grain of Mo in the supercell of the pure $\Sigma 5$ STGB was replaced by MoC. A previous study[30] yielded an equilibrium volume of 0.0419 nm^3 and a c/a ratio of 1.39 (c=0.432 nm and a =0.311 nm) for bct MoC. To cope with the lattice mismatch between this carbide and bcc Mo and to maintain the coherency of the interface, the carbide phase was compressed to $\tilde{a}$=0.956 a_0 while keeping the c/a ratio fixed. This corresponds to a compression of the tetragonal unit cell by 13% to a volume of 0.0364 nm^3. With this lattice constant, the two model interfaces shown in Fig. 6 were constructed. The translation state of the phase boundary was then determined by rigid grain shifts along the [001], [$\bar{1}$30], and [310] directions with respect to the Mo grain, followed by relaxation of all atomic positions.

The shifts along [310] lead to an interfacial excess expansion perpendicular to the grain boundary. The corresponding energy curves are shown in Fig. 7. Displayed is the negative work of separation $-W_{sep}$ calculated according to Eq. (6).

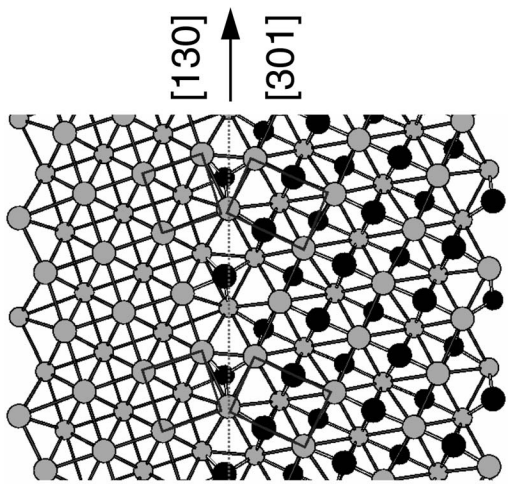

FIG. 8. Interface I after volume expansion and relaxation of all atomic positions. The large atoms are positioned in the paper plane, and the small atoms in the next layer in the [001] direction. Mo atoms are gray, and C atoms black. Compared to the geometric construction, the supercell is expanded by 17% of a_0 perpendicular to the interface and the C atoms of the first layer next to the grain boundary are relaxed into the interface layer.

For interface I, the minimum is located at a total volume of 0.3658 nm^3, corresponding to an expansion perpendicular to the interface of 17.5% of a_0=0.313 nm, the bulk lattice constant of bcc Mo. A closer inspection of the relaxed coordinates shows that the volume change takes place almost completely at the interface. It originates from a migration of the first layer of C atoms in MoC adjacent to the interface into the boundary plane, as visible in Fig. 8. The C atoms moved from their original octahedral sites to the centers of the trigonal prisms formed by Mo atoms at the grain boundary, which had been determined to be the most favorable positions for interstitial impurities. In the resulting configuration, the adjacent planes are almost at equal distance to the grain boundary. The interplanar spacings between the grain boundary and the adjacent MoC (103) [Mo (310)] planes amount to 0.133 and 0.132 nm, respectively. These distances represent a compression of the lattice spacing in MoC by 16% with respect to the bulk value and an expansion of the lattice spacing in Mo by 34%. Both can be explained by the migration of C to the boundary.

At interface II, the trigonal prism does not exist as structural unit at the boundary. Thus, the C atoms remain inside the MoC grain and the relaxation effects are less pronounced. The minimum of the energy-volume curve is located at 0.3652 nm^3, corresponding to an expansion of 16.8% of a_0. Again, a deviation from the distances in the bulk phases is almost completely restricted to the interface and its neighboring planes. Now, the interplanar spacing between the grain boundary and the adjacent Mo (310) [MoC (103)] plane amounts to 0.127 and 0.112 nm, respectively. This corresponds to an expansion of the Mo-Mo interplanar distance of 29% with respect to bulk Mo and a compression of the interplanar spacing of 9% with respect to bulk MoC.

On the minimum energy configurations of the two interfaces I and II, rigid grain shifts were imposed along $[\bar{1}30]$ and [001] to probe the structural stability. The respective energies versus shifts are shown in Fig. 9. For both interfaces, when relaxations of the atomic positions are allowed at the points marking the shifts along $[\bar{1}30]$ and [001], the structures relax back to the common minimum of the curves. This means that the Mo/MoC interfaces, as constructed in Fig. 6, are indeed stable against a relative shift of grains parallel to the interface. This is unlike the behavior of the pure $\Sigma 5$ STGB of Mo, where at a shift of 18% of a_0 along [001] a stable translation state breaking the mirror symmetry of the interface was found.[7] An explanation for this was given in Ref. 1 in terms of the directional Mo-C bonds across the interface which make a symmetric configuration preferable.

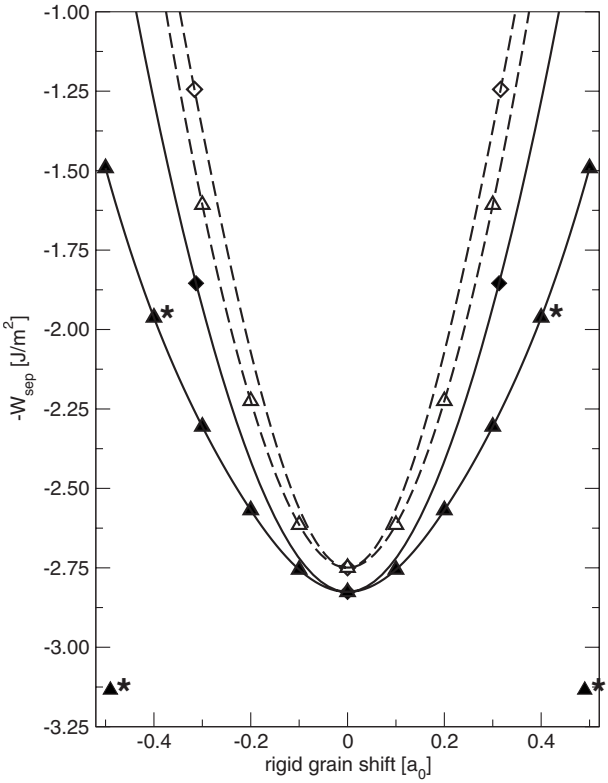

FIG. 9. Negative work of separation $-W_{sep}$ for interface I (full symbols) and interface II (open symbols), for grain shifts along [001] (triangles) and [−130] (diamonds) (directions refer to the Mo grain). Note that a shift of 40% a_0 along the [001] direction at interface I and subsequent relaxation of the atomic positions leads to a new configuration with a very low work of separation, labeled by the star. Details are given in the text.

In the case of interface I, a further stable translation state occurs for large shifts along [001]. This phenomenon will be discussed below. First, the relaxed structures of interfaces I and II are characterized by their interface energies and works of separation, in comparison with the corresponding values for the third kind of interface considered, the MoC STGB.

B. Model structures: The MoC symmetrical tilt grain boundary

If one assumes a precipitation of MoC in a symmetric fashion with respect to the $\Sigma 5$ STGB in Mo (cf. Fig. 3), one

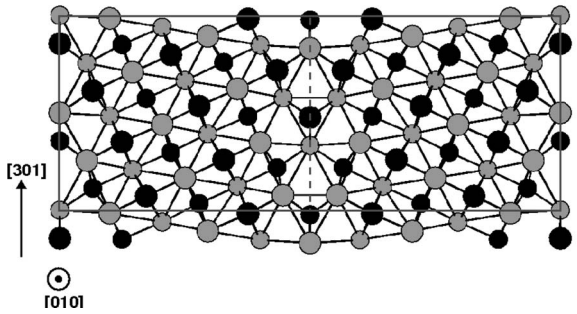

FIG. 10. Supercell of a STGB in tetragonal MoC after relaxation of all atomic positions. The large atoms are positioned in the paper plane, and the small atoms in the next layer in the [010] direction. Mo atoms are gray, and C atoms black.

arrives at a precipitate containing a (310)[001] STGB with 1 ML of C at the interface and a C-deficient adjacent layer on each side. The precipitate is limited by two interfaces II. In analogy with splitting the asymmetric precipitate (cf. Fig. 4) in two model supercells containing interfaces I and II, respectively (cf. Fig. 6), the symmetric precipitate was modeled by splitting the problem into two interfaces II and the MoC STGB. The supercell containing the MoC grain boundary was constructed assuming the same dimensions parallel to the interface as for the Mo STGB and by choosing the bulk value $c/a=1.39$. All atomic positions were relaxed until the forces were negligible (less than 10^{-3} Ry/bohr ≈ 0.26 eV/nm). The relaxed structure is shown in Fig. 10.

C. Interface energies

The interface energies for Mo/MoC interfaces I and II as well as for the STGB in Mo and MoC, which are listed in Table II, were calculated by using either the chemical potentials μ_{Mo}^{bcc} and $\mu_{\mathrm{C}}^{diamond}$ for the complete supercell (γ) or by using the chemical potential μ_{Mo}^{bcc} for the Mo grain (if present) and the energy of a formula unit of MoC in tetragonal MoC for the MoC grain (if present, γ'). γ'_{corr} includes a correction term, which is the elastic energy difference between the equilibrium volume and the volume of a laterally compressed unit cell (to match the lattice of Mo at the interface) of tetragonal MoC, multiplied by the number of unit cells in the carbide film.

The works of separation were calculated in a similar manner. The results are listed in Table III. The values compare well with adhesive energies from other DFT studies of metal/carbide interfaces in the literature.[31–33] Both the interface energies and the works of separation show that the asymmetric precipitate, i.e., the sum of the energies of interfaces I and II, is considerably more favorable than the symmetric precipitate containing the MoC STGB because of its high interface energy and low work of separation. This is in agreement with experimental observations.[2] The characteristic energies of interfaces I and II do not differ significantly of the respective values for the pure Mo STGB. Thus, the precipitate does not alter the adhesive strength of the material. It is likely, however, that it has a strong influence on the deformability of the system since the mobility of the Mo/MoC interface and its resistance to interfacial sliding should differ significantly from that of the Mo STGB. These processes are complex and their description is beyond the scope of this paper. However, some preliminary findings are given in the following.

TABLE II. Interface energies after Eq. (3), calculated with $\mu_{\mathrm{Mo}}=\mu_{\mathrm{Mo}}^{bcc}$ and $\mu_{\mathrm{C}}=\mu_{\mathrm{C}}^{diamond}$ (γ) and referred to bcc bulk Mo and tetragonal bulk MoC without (γ') and with (γ'_{corr}) corrected elastic strain contribution for MoC. (IF I and IF II denote interface I and interface II, respectively.)

	IF I	IF II	MoC STGB	Mo STGB
γ (J/m^2)	1.937	2.089	4.112	1.807
γ' (J/m^2)	−1.001	−0.846	−1.171	1.807
γ'_{corr} (J/m^2)	1.672	1.827	3.636	1.807

TABLE III. Work of separation after Eq. (6). (IF I and IF II denote interface I and interface II, respectively, and ms means mirror symmetric.)

	IF I	IF II	MoC STGB	Mo STGB (ms)
W_{sep} (J/m^2)	5.643	5.491	3.909	5.788
$W_{sep,corr}$ (J/m^2)	2.973	2.820	−0.872	

D. Grain boundary migration

A large relative shift of the Mo and MoC grains along [001], namely, by a value between 30% and 40% of a_0, initiates an interfacial sliding process accompanied by grain boundary migration. Relaxation of the atomic positions leads to a final relative shift parallel to the interface of nearly 50%. Furthermore, as visible in the picture of the resulting relaxed structure in Fig. 11, the Mo/MoC interface is moved perpendicular to the [001] direction of the translation, by one

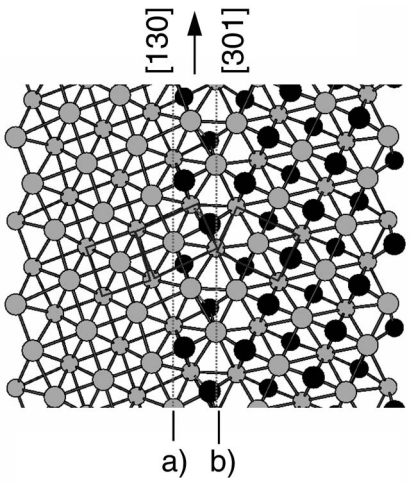

FIG. 11. Interface I after shift to point * in Fig. 9 and subsequent relaxation of the atomic positions. The large atoms are positioned in the paper plane, and the small atoms in the next layer in the [001] direction. Mo atoms are gray, and C atoms black. (a) The Mo/MoC interface moved into the Mo grain, and (b) a new grain boundary occurs inside the MoC grain.

atomic layer along [310] into the Mo grain. Thus, a grain boundary inside MoC evolves. The underlying atomistic process is the following: by displacing the grains, the C atom at the grain boundary was pushed from its interstitial site in the trigonal prism across the grain boundary onto an octahedral site in the Mo grain. At the same time, a neighboring C atom moved from an octahedral site in the carbide on the trigonal prism site. This state is lower in energy because, now, more C atoms occupy interstitial sites close to the grain boundary, which provide more space than in compressed MoC. This process is a possible explanation of the experimental finding of a not well defined, sharp interface of type II (Ref. 2): even if the precipitate grows asymmetrically into one grain and is thus clearly limited by the former $\Sigma 5$ grain boundary, displacements of small amounts of carbon across the interface may smear out this sharp boundary to some extent. Furthermore, the underlying atomistic mechanism can be triggered repeatedly, for example, by applying mechanical stress parallel to the grain boundary. Thus, a STGB in MoC, as in the case of the symmetric precipitate, can evolve. The motion of grain boundaries in terms of a combined sliding and migration process has been observed and investigated both experimentally[34] and computationally[35] in pure metals. However, to the authors' knowledge, it has not yet been described for heterophase interfaces in the literature. A validation experiment for this prediction may be difficult but would be very desirable.

From Fig. 9, the energy barrier for this combined sliding and migration mechanism can be roughly estimated to be $0.5-0.8\ \mathrm{J/m^2}$. A more detailed investigation of the respective processes is promising to judge the influence of the precipitate and the grain boundary migration on the material's stability and ductility.

VII. SUMMARY AND CONCLUSION

We have studied nucleation and growth of a tetragonal MoC precipitate at a $\Sigma 5$ STGB in Mo at the atomic scale. Our results show the tendency of the carbide phase to grow with the tetragonal distortion forming an angle of 108° with the grain boundary, in agreement with experimental observations.[2] The saturation concentration of C in the grain boundary plane as well at its tendency to segregate to the interface between the precipitate and the Mo matrix can be manipulated by the chemical potential of carbon.

The characterization of two Mo/MoC phase boundaries and a MoC STGB shows the tendency of the precipitate to grow in an asymmetric fashion with respect to the original Mo grain boundary. The energies of interfacial adhesion at the pure grain boundary and in the resulting Mo/MoC system are comparable, i.e., the interfacial precipitate in this boundary configuration does not significantly reduce interfacial cohesion. However, mechanical load can induce the migration of the interface into the carbide, leading to a high-energy grain boundary with a low work of separation, i.e., a very brittle interface. The underlying process of the grain boundary migration, the diffusion of carbon across the interface, can explain the experimental finding of a not atomically sharp interface of type II.[2]

It shall be mentioned that misfit dislocations, which will play an important role in the case of an extended precipitate, have not been considered in this work because the investigation of dislocations is out of the scope of an *ab initio* calculation. However, the coherent, strained precipitate modeled in the study at hand corresponds well to the thin film of MoC_x observed experimentally. The contribution of the misfit strain to the ideal work of fracture has been accounted for by calculating an elastic correction energy to the work of separation. Yet, it would be interesting to see the effect of dislocation emission on the stress field near the tip of a crack propagating close to the Mo/MoC_x interface. We postpone this as a topic for a large-scale atomistic simulation with suitable interatomic potentials for Mo-MoC systems.

[1] R. Janisch and C. Elsässer, Phys. Rev. B **67**, 224101 (2003).
[2] J. M. Pénisson, M. Bacia, and M. Biscondi, Philos. Mag. A **73**, 859 (1996).
[3] K. Morita and H. Nakashima, Mater. Sci. Eng., A **1053**, 234 (1997).
[4] G. H. Campbell, J. Belak, and J. A. Moriarty, Scr. Mater. **43**, 659 (2000).
[5] A. G. Marinopoulos, V. Vitek, and A. E. Carlsson, Philos. Mag. A **72**, 1311 (1995).
[6] M. Bacia, J. Morillo, J. M. Pénisson, and V. Pontikis, Philos. Mag. A **76**, 945 (1997).
[7] T. Ochs, O. Beck, C. Elsässer, and B. Meyer, Philos. Mag. A **80**, 351 (2000).
[8] T. Ochs, C. Elsässer, M. Mrovec, V. Vitek, J. Belak, and J. Moriarty, Philos. Mag. A **80**, 2405 (2000).
[9] R. Janisch, T. Ochs, A. Merkle, and C. Elsässer, *Multiscale Phenomena in Materials—Experiments and Modeling*, MRS Symposia Proceedings No. 578 (Materials Research Society, Pittsburgh, 2000), p. 405.
[10] J.-M. Jardin, A. Kobylanski, and C. Goux, C. R. Hebd. Seances Acad. Sci., Ser. A B, Sci. Math. Sci. Phys **280**, 717 (1975).
[11] D. Lepski and P. Burck, Phys. Status Solidi A **64**, 625 (1981).
[12] D. Lepski and P. Burck, Phys. Status Solidi A **70**, 571 (1982).
[13] C. Elsässer, N. Takeuchi, K.-M. Ho, C. T. Chan, P. Braun, and M. Fähnle, J. Phys.: Condens. Matter **2**, 4371 (1990).
[14] C. Elsässer, Ph.D. thesis, Universität Stuttgart, 1990.
[15] K. M. Ho, C. Elsässer, C. T. Chan, and M. Fähnle, J. Phys.: Condens. Matter **4**, 5207 (1992).
[16] B. Meyer, Ph.D. thesis, Universität Stuttgart, 1998.
[17] B. Meyer, F. Lechermann, C. Elsässer, and M. Fähnle, FORTRAN90, program for mixed-basis pseudopotential calculations for crystals, Max-Planck-Institut für Metallforschung Stuttgart.
[18] B. Meyer, K. Hummler, C. Elsässer, and M. Fänle, J. Phys.: Condens. Matter **7**, 9201 (1995).
[19] F. Lechermann, F. Welsch, C. Elsässer, C. Ederer, M. Fähnle, J. M. Sanchez, and B. Meyer, Phys. Rev. B **65**, 132104 (2002).
[20] J. P. Perdew and A. Zunger, Phys. Rev. B **23**, 5048 (1981).

[21] D. R. Hamann, M. Schlüter, and C. Chiang, Phys. Rev. Lett. **43**, 1494 (1979).
[22] D. Vanderbilt, Phys. Rev. B **32**, 8412 (1985).
[23] C. Elsässer, O. Beck, T. Ochs, and B. Meyer, *Microscopic Simulation of Interfacial Phenomena in Solids and Liquids*, MRS Symposia Proceedings No. 492 (Materials Research Society, Pittsburgh, 1998), p. 121.
[24] J. Moreno and J. M. Soler, Phys. Rev. B **45**, 13891 (1992).
[25] I. G. Batyrev, A. Alavi, and M. W. Finnis, Phys. Rev. B **62**, 4698 (2000).
[26] M. W. Finnis, J. Phys.: Condens. Matter **8**, 5811 (1996).
[27] J. W. Gibbs, *The Scientific Papers of J. William Gibbs* (Dover, New York, 1961).
[28] E. D. Hondros and M. P. Seah, Metall. Trans. A **8**, 1363 (1977).
[29] E. D. Hondros, Proc. R. Soc. London, Ser. A **286**, 479 (1965).
[30] R. Janisch, Ph.D. thesis, Universität Stuttgart, 1999.
[31] A. Arya and E. A. Carter, J. Chem. Phys. **118**, 8982 (2003).
[32] M. Christensen and G. Wahnström, Acta Mater. **52**, 2199 (2004).
[33] D. J. Siegel, L. G. Hector, Jr., and J. B. Adams, Surf. Sci. **498**, 321 (2002).
[34] M. Winning, G. Gottstein, and L. S. Shvindlerman, Acta Mater. **49**, 211 (2001).
[35] C. Molteni, N. Marzari, M. C. Payne, and V. Heine, Phys. Rev. Lett. **79**, 869 (1997).
[36] Note that there are always two equivalent interfaces in the supercell because of the periodic boundary conditions. Therefore, always two C atoms are added to equivalent interstitial sites.